DESIGN OF THE MAIN MAGNETS OF THE SESAME STORAGE RING

A. Milanese[1], E. Huttel[2], M. Shehab[2]
[1] CERN, Genève, Switzerland, [2]SESAME, P.O. Box 7, Allan 19252, Jordan

Abstract

This paper describes the magnetic design of the main magnets of the SESAME storage ring. The 16 dipoles are combined function bending magnets, designed with an adjustable iron shimming scheme. The 64 quadrupoles are of two different lengths and strengths. The 64 sextupoles are optimized for field quality in 3D without end pole chamfers and they include additional coils to provide a horizontal / vertical dipole and a skew quadrupole terms.

INTRODUCTION

SESAME (Synchrotron-light for Experimental Science and Applications in the Middle East) is an electron light source under construction in Jordan [1]. The accelerator complex comprises a 22.5 MeV microtron, a 800 MeV booster, and a 2.5 GeV storage ring. The main ring has a circumference of 133.2 m and it provides a horizontal emittance (rms) of 26 nm·rad at top energy.

The lattice of the storage ring is based on a Double Bend Achromat (DBA) scheme [2]. The ring consists of 16 identical half-cells, with a central combined function (bending and defocusing gradient) magnet (BM), 2 focusing quadrupoles (QF), 2 defocusing quadrupoles (QD), and 4 sextupoles (2 SF and 2 SD), with embedded correctors. The combined function magnets perform most of the vertical focusing, that is complemented by the QD quadrupoles. All the magnets of a half-cell are mounted on a single common girder.

In the next sections the different families of magnets are described with their peculiarities. In all cases the electromagnetic design is carried out with the help of magnetic simulations in Opera [3].

BENDING MAGNETS

Several light sources have combined function magnets, for example ALBA, ALS, ASP, CLS, ELETTRA, SPEAR3 [4-6]. Considering the specific requirements of SESAME in terms of gap, bending angle, field, gradient, and overall integration, a dedicated design is carried out.

The magnetic cross section is shown in Figure 1. The C geometry allows a convenient extraction of the emitted radiation. The pole profile is optimized for field quality, as follows. The theoretical hyperbolic profile is given by

$$y = \frac{B_c h}{B_c + G_c x},$$

where B_c and G_c are central field and gradient and h is the half-gap. For convenience, instead of the theoretical profile, a circular arc of radius R_{pole} inclined of α_{pole} with respect to the midplane is used. At first order, the angle α_{pole} is proportional to the gradient G_c, as

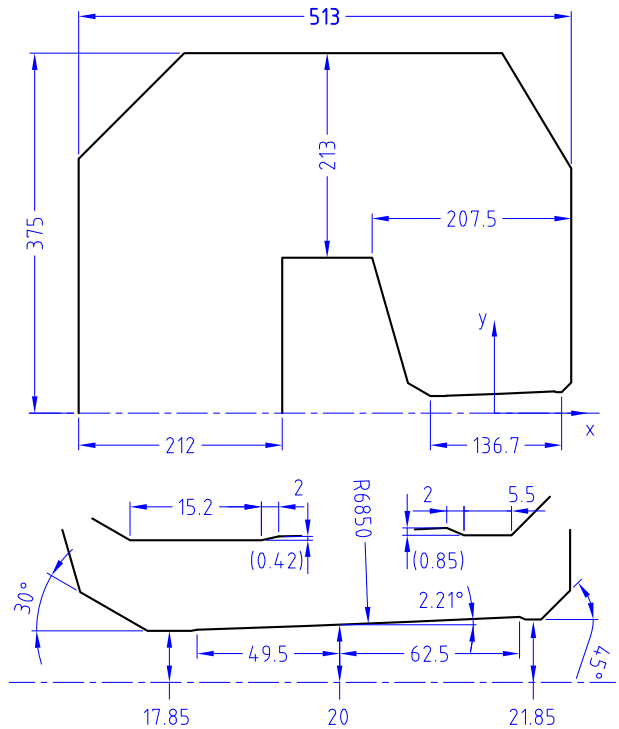

Figure 1: Cross section (1/2) of the bending magnets.

$$\alpha_{pole} \cong -\frac{G_c h}{B_c} = 2.20°.$$

The radius R_{pole} acts on the sextupole component and as a first guess the central curvature radius of the hyperbole,

$$\frac{B_c^2}{2hG_c^2} = 6803 \text{ mm},$$

can be taken. The actual values of α_{pole} and R_{pole} are obtained with finite element simulations and they are very close to the theoretical estimates shown above. At both ends of the circular arc two flat shims are present, to shape the field quality towards the borders of the aperture, and to be used as mechanical reference features.

The optimization aims at field quality from injection to top energy. Furthermore, the tapered profile of the pole produces a gradual filling of flux density at 2.5 GeV along the width of the pole, in such a way that the field profile in the midplane is somehow independent from the actual iron BH curve.

The average field at nominal condition in the return legs is 1.5-1.6 T, resulting in a 2D efficiency of 98%. This refers to a low Si grade electrical steel, like M1200-100A. For higher Si grades, like M270-50A, the efficiency is lower, at 94%. This is related to the earlier saturation onset.

As for the 3D design, the magnets are curved and with parallel end plates. The termination of the poles is important, as it drives the edge effects at the entrance / exit of the magnets, in a region particularly affected by saturation. Similar combined function magnets of other synchrotron sources have adopted different strategies for the pole ends. In ELETTRA, for example, the poles were machined in a vertical lathe; then, individual shims embedded in a brass holder were added after magnetic measurements [6]. In ALBA and CLS, a chamfer including a pole face rotation was used [4,5]. Here we propose a hybrid solution, based on three stacks of shims to be accommodated in a cut-out of the end plate. The vertical height of the shims is 20 mm and up to 20 shims (1 mm each) can be stacked, as shown in Figure 2. This allows individual shimming as an extra mean to attain magnet-to-magnet reproducibility and integrated field quality, in particular sextupole component. On the other hand, the step-like profile approximates an inclined chamfer (including a pole face rotation), to achieve the desired field and gradient distribution in 3D, also in the end regions of the magnet.

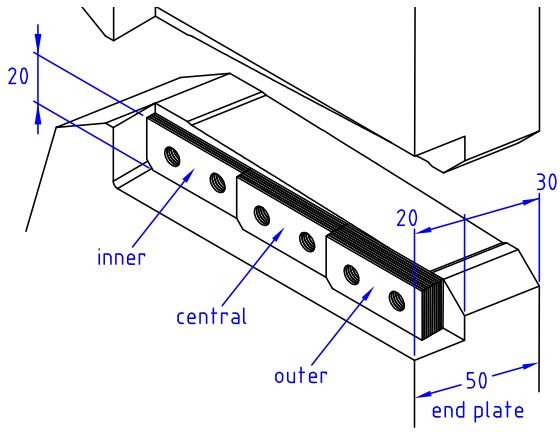

Figure 2: End pole shimming of the bending magnets.

Table 1: Main Parameters of the Combined Function Bending Magnets, 2.5 GeV Operation

Number of magnets	16
Bending radius [mm]	5729.58
Bending angle [deg]	22.5
Central field [T]	1.455
Field gradient [T/m]	-2.79
Central vertical gap (total) [mm]	40
Magnetic length [mm]	2250
Current [A]	494
Number of turns (total)	96
Conductor size [mm]	13 × 11, ⌀ 6
Current density [A/mm^2]	4.3
Number of pancakes	8
Resistance (total) [mΩ]	83
Inductance (total) [mH]	145
Power [kW]	20.2
Water temperature rise [°C]	10
Pressure drop [bar]	7.0
Flow rate / magnet [l/min]	29.0

The main parameters of the bending magnets are summarized in Table 1. As material for the magnetic yoke, 1 mm thick electrical steel with low Si content, grade M1400-100A, is used for the laminations, and pure iron for the end plates. All 16 dipoles are connected in series and powered by a single power converter.

QUADRUPOLES

Considering the requirements in terms of strength and apertures, the QF and QD quadrupoles can use the same lamination geometry (Figure 3). The pole tip geometry is made of a circular arc and of straight lines. A segment parallel to the midplane is included to ease precise assembly and dimensional checks. A 0.5 mm fillet (not shown in the sketch) is added in all corners.

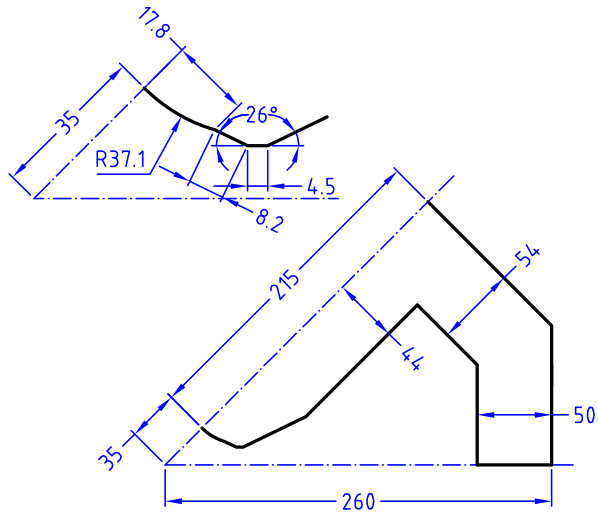

Figure 3: Cross section (1/8) of the quadrupoles, with detail of the pole tip geometry.

Table 2: Main Parameters of the Quadrupoles @ 2.5 GeV

	QF	QD
Number of magnets	32	32
Field gradient [T/m]	16.5	-7.6
Aperture radius [mm]	35	
Field at pole tip [T]	0.58	0.27
Magnetic length [mm]	308	135
Current [A]	238	195
Number of turns (per pole)	34	19
Conductor size [mm]	8.5 × 8.5, ⌀ 4	
Current density [A/mm^2]	4.0	3.3
Resistance (total) [mΩ]	38	12
Inductance (total) [mH]	21	3
Power [kW]	2.1	0.4
Water temperature rise [°C]	5	5
Pressure drop [bar]	5.0	5.0
Flow rate / magnet [l/min]	6.1	1.4

The pole tip geometry is optimized in 2D for field quality. The first allowed harmonics – in units of 10^{-4} with respect to the main field, and at a radius of 24 mm – are $b_6 = 0.1$, $b_{10} = 0.2$ and $b_{14} = 0.4$. In 3D a 45° chamfer is

ISBN 978-3-95450-132-8

introduced in the pole tip ends to cancel the integrated dodecapole. Considering the different lengths and nominal strengths of the quadrupoles, simulations suggest 5.7 × 5.7 mm chamfers for QF and 5.3 × 5.3 mm for QD.

The main parameters of the quadrupoles are summarized in Table 2. Each quadrupole magnet will be powered by an individual power converter. For the magnetic yoke, 1 mm thick laminations of electrical steel are used, grade M1300-100 A.

SEXTUPOLES

The SF and SD sextupoles are the same magnets, apart from the polarity.

Since the bore is large compared to the length, the field quality is optimized directly in 3D. To avoid machining the classical end pole tip chamfers, the first allowed harmonic b_9 is cancelled in 3D by introducing a bias in 2D – of the order of $12.8 \cdot 10^{-4}$ at 24 mm – and by exploiting the edge effect of straight sextants. The resulting pole tip geometry – shown in Figure 4 together with the cross section – is made of a circular arc and of straight lines, with a segment parallel to the midplane to ease precise assembly and dimensional checks. Fillets of 0.5 mm radius are present in all corners, but on the very edge, where a 1 mm fillet is used instead. The nominal parameters of the sextupoles are reported in Table 3.

As in several synchrotron sources, such as ALBA, ALS and SOLEIL [7, 8] a horizontal dipole, vertical dipole and skew quadrupole corrector are superimposed on top of the sextupole, for compactness. This is obtained by additional winding on the poles. The powering scheme follows the classical analysis of Halbach [9]. The integrated strengths are checked with 3D simulations, as in this case the magnetic length of the yoke when used in a dipole or quadrupole configuration is considerably longer than when used in a sextupolar way. The nominal parameters of the correctors are reported in Table 4. The kick of the corrector dipoles corresponds to 0.5 mrad at 2.5 GeV.

To make the correctors work comfortably in a orbit feedback loop up to 100 Hz, a 0.5 mm thick high Si electrical steel, grade M270-50A, is used.

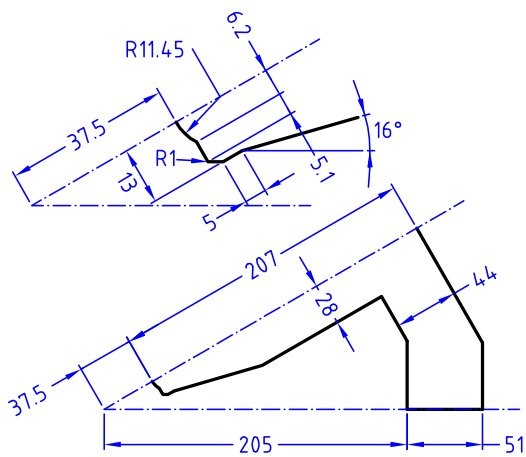

Figure 4: Cross section (1/12) of the sextupoles, with detail of the pole tip geometry.

Table 3: Main Parameters of the Sextupoles @ 2.5 GeV

	SF	SD
Number of magnets	32	32
Sextupole strength [T/m^2]	63.4	-108.9
Aperture radius [mm]	37.5	
Field at pole tip [T]	0.09	0.15
Magnetic length [mm]	123	
Current [A]	60	103
Number of turns (per pole)	15	
Conductor size [mm]	6.5 × 6.5, ⌀ 3.5	
Current density [A/mm^2]	1.9	3.2
Resistance (total) [mΩ]	23.8	
Inductance (total) [mH]	2.9	
Power [W]	86	252

Table 4: Nominal Parameters of the Correctors

	VD	HD	SQ
Integrated strength	4.16 mTm	4.16 mTm	90 mT
Current [A]	10	8	19
Number of turns (per pole)	80 / 40	80	40
Conductor size [mm]	3.75 × 1.6		
Current density [A/mm^2]	1.7	1.3	3.2
Resistance (total) [mΩ]	388	374	106
Inductance (total) [mH]	17	23	3.8
Power [W]	35	23	40

ACKNOWLEDGEMENTS

The authors thank M. Attal, J. P. Koutchouk, F. Makahleh, A. Nadji, H. Tarawneh, D. Tommasini for fruitful discussions and support.

This work is supported by the European Commission and CERN under the CESSAMag project, FP7 contract no. 338602.

REFERENCES

[1] SESAME website, www.sesame.org.jo
[2] G. Vignola and M. Attal, "SESAME lattice," SESAME Technical Note O-1, Dec. 2004.
[3] "Opera-2d and Opera-3d User Guides and Reference Guides," Vector Fields, Nov. 2011.
[4] D. Einfeld et al., TUPMN068, Proc. PAC'07, Albuquerque, NM (2007); http://JACoW.org
[5] L. Dallin et al., TUPLE054, 2340, Proc. EPAC'02, Paris, France (2002); http://JACoW.org
[6] G. Petrucci and D. Tommasini, p. 2820, Proc. PAC'93, Washington, DC (2003); http://JACoW.org
[7] S. Marks, "Magnetic Design of Trim Excitations for the Advanced Light Source Storage Ring Sextupole," IEEE Trans. of Magn. 32, 2077 (1996).
[8] A. Nadji, J. Neel, P. Peaupardin, TUP06, p. 1954, Proc. EPAC'98, Stockholm, Sweden (1998); http://JACoW.org
[9] K. Halbach, "First order perturbation effects in iron-dominated two-dimensional symmetrical multipoles," NIM 74, 147 (1969).